



ORIGINAL RESEARCH

Biomimetic preparation and multi-scale microstructures of nano-silica/polyurethane elastomeric fibers

Quanyong Liu^{a,*}, Li Gao^a, Lei Jiang^{a,b,**}

^aKey Laboratory of Bio-Inspired Smart Interfacial Science and Technology of Ministry of Education, Beijing Key Laboratory of Bio-inspired Energy Materials and Devices, School of Chemistry and Environment, Beihang University, Beijing 100191, China

^bBeijing National Laboratory for Molecular Sciences (MNLMS), Key Laboratory of Organic Solids, Institute of Chemistry, Chinese Academy of Sciences, Beijing 100190, China

Received 13 June 2013; accepted 26 November 2013

Available online 27 December 2013

KEYWORDS

Biomimetic preparation;
Elastomeric fiber;
Nano-silica;
Polyurethane;
Microstructure;
Self-assembly

Abstract Bioinspired by the spinning of spider silks, the biomimetic preparation of nano-silica/polyurethane (nano-SiO₂/TPU) elastomeric fibers with distinctive multi-scale microstructures was successfully implemented. The formation mechanism of the nano-SiO₂/TPU fibers was considered as the integrated mechanism of diffusion, coagulation, self-assembly, and microphase separation, same as that of the native spider silks. The mass ratio of nano-SiO₂ to TPU greatly influenced the external and inner microstructures of the nano-SiO₂/TPU fibers. The formation process of the nano-SiO₂/TPU fibers was simply described as three main stages, and the second stage, such as the adding of the ethanol solvents and nano-SiO₂ in different diameters, was thought to be very crucial for the final external and inner microstructures of the prepared fibers. For example, the adding of the ethanol and the nano-SiO₂ spheres in diameter of 10 nm resulted in the existence of many TPU-self-assembled microspheres mostly spaced apart by the nano-SiO₂ aggregates in the nano-SiO₂/TPU fibers, while the adding of the ethanol and the nano-SiO₂ spheres in diameter of 100 nm resulted in the existence of the nano-SiO₂ spheres, instead of the TPU-self-assembled microspheres, distributed in the nano-SiO₂/TPU fibers.

© 2013 Chinese Materials Research Society. Production and hosting by Elsevier B.V. All rights reserved.

*Corresponding author. Tel.: +86 10 82316160.

**Corresponding author at: Key Laboratory of Bio-Inspired Smart Interfacial Science and Technology of Ministry of Education, Beijing Key Laboratory of Bio-inspired Energy Materials and Devices, School of Chemistry and Environment, Beihang University, Beijing 100191, China. Fax: +86 10 82621396 (L. Jiang).

E-mail addresses: liu_quanyong@buaa.edu.cn (Q. Liu), jianglei@iccas.ac.cn (L. Jiang).

Peer review under responsibility of Chinese Materials Research Society.



Production and hosting by Elsevier

1. Introduction

Living things (e.g., animals and plants) have evolved for billions of years to achieve special functions, such as superhydrophobicity, self-cleaning, structural color, anti-reflection, anti-fogging, anti-biofouling, drag reduction, reversible adhesion, thermal insulation, mechanical reinforcement, and self-repair [1–3]. When a special function needs to be effectively executed, the biomaterials from the living things usually play vitally important roles because of the materials' unique microstructures [4–7].

Especially for example, the native spider silks, a kind of natural biomaterials having been proposed for use in various fields [8,9], are essentially the bioelastomer fibers [10–12] with perfect multi-scale microstructures [13–17] (e.g., the protein nano-crystalline reinforced amorphous phase of dragline silks [13,16] and periodic helix of capture silks [17]), presenting many attractive functions such as excellent mechanical properties [18–20], remarkable damping capacity [21], extraordinary shape memory [22], directional water collection [17], outstanding biosorption ability [23], suitable biocompatibility [24], and exceptionally high thermal conductivity [25]. Here, particularly, we hope to indicate a point that the perfect multi-scale microstructures of the native spider silks chiefly rely on the unique spinning process consisting of the gradual self-assembly of silk proteins in vivo and subsequent stretching and drying of protein silks in vitro [19,26].

Directly learning from the multi-scale microstructures of the native spider silks, the researchers have designed many bioinspired materials with distinctive structures and functions [27–33]. In the designs of those bioinspired materials, the preparation methods, like the spinning process of the native spider silks, seemed to be very significant. Naturally, an interesting challenge came into being whether we could directly mimic the spinning process of the native spider silks to prepare an elastomeric fiber with multi-scale microstructures by only using polymer materials. Of course, the answer is yes, and we have successfully realized the biomimetic preparation of three elastomeric fibers with unique micro/nano structures on the surfaces by using the organic polymer nanoparticles of ultrafine full-vulcanized powdered nitrile-butadiene rubbers (UFPNBR nanoparticles, about 100 nm in diameter) and thermoplastic polyurethane (TPU) elastomers [34]. The first UFPNBR/TPU fiber was only decorated by the micron-sized grooves on the surface, and the second UFPNBR/TPU fiber was dotted by both the micron-sized grooves and nanometer-sized spheres on the surface, while the third UFPNBR/TPU fiber was helical and with a concave–convex surface.

However, in the preparation of the UFPNBR/TPU fibers with multi-scale microstructures, some shortcomings potentially existed. First, the cross-linked polymer nanoparticles were easily aged because of the high specific surface areas and many active groups in structures, and this caused their properties easily changed with time during storage. Second, the cross-linked polymer nanoparticles usually consisted of sols and gels because of the restriction of imperfect crosslinking in production, and this resulted their dimensions were unstable in organic solvents during treatment. Third, the cross-linked polymer nanoparticles enjoyed aggregating into big microspheres without the interfaces of nanoparticles because of the strong interaction among macromolecules and the self-ligation of sols in composition, and this led their homogeneous dispersion in matrixes seemed to be unattainable during mixing. Fourth, the UFPNBR/TPU fibers very possibly presented a limited tensile strength because of the limited reinforcement effect of the cross-linked polymer nanoparticles with low crystallinity. All these shortcomings might slightly restrain the prospective functions and applications of the UFPNBR/TPU fibers.

In order to further enrich the categories of this fibers, in the work, we attempted to use inorganic silica nanoparticles (nano-SiO₂ spheres with diameter of 10 nm and 100 nm), instead of the UFPNBR nanoparticles, to prepare the nano-SiO₂/TPU elastomeric fibers by the same preparation method. The nano-SiO₂ spheres were expected, together with the TPU macromolecules and like the protein micelles (about 10–100 nm in diameter) formed in the spinning of the native spider silks [26], to self-assemble into

distinctive multi-scale microstructures on and in the nano-SiO₂/TPU fibers.

2. Experimental

2.1. Materials

The TPU elastomer (Elastollan® 1180A, 1.11 g cm⁻³ in density), with outstanding hydrolysis resistance and low temperature flexibility, was obtained from the BASF group. The nano-SiO₂ spheres (nanopowder, spherical and porous, about 10 nm in diameter, about 590–690 m²/g surface areas) were bought from the Sigma-Aldrich Company, while the nano-SiO₂ spheres (solid powder, spherical and imporous, about 100 nm in diameter, about 10–20 m²/g surface areas) were gotten from the Institute of Chemical Technology of the Chinese Academy of Sciences. The nanoparticles of ultrafine full-vulcanized powdered nitrile-butadiene rubbers (UFPNBR, VP-401, about 100 nm in diameter, above 90% in gel fraction) were achieved from the SINOPEC Beijing Research Institute of Chemical Industry. N,N-dimethyl formamide (above 99.5% in purity and 0.945–0.950 g cm⁻³ in density) and ethanol (above 99.7% in purity and 0.887–0.889 g cm⁻³ in density) were obtained from the Beijing Chemical Works in China. All these materials and reagents were used as received.

2.2. Preparation of the spinning dopes

Firstly, the TPU solution with N,N-dimethyl formamide (DMF) as solvents was prepared, and the solution concentration was controlled at 0.2 g/mL (the ratio of TPU mass to DMF volume). Secondly, a certain amount of nanoparticles (nano-SiO₂ or UFPNBR) were wetted by using a determined volume of ethanol solvents and ultrasonically dispersed for 10 min in a reagent bottle, and the mass ratios of nanoparticle to TPU were controlled at 0/20, 1/20, 2/20, 3/20, 4/20, and 5/20. Thirdly, the wetted and dispersed nanoparticles, together with the used ethanol, were poured into the prepared TPU solutions, and the residual nanoparticles in the reagent bottle were cleaned up by using a determined volume of DMF and also poured into the TPU solutions. The volume of the secondly used DMF was the same as the volume of the used ethanol, and at that time the TPU solution concentration was changed from the initial 0.2 g/mL into the final 0.1 g/mL (the ratio of TPU mass to total volume of DMF and ethanol). Fourthly, the TPU solutions including nanoparticles were magnetically stirred for 2 h to obtain the required homogeneous spinning dopes. The composition of the final spinning dopes was listed in Table 1.

2.3. Preparation of the fibers

As described in the previous study [34], first, the prepared spinning dopes were stored in a container with piston and pressed very slowly into an artificial spinning duct (about 500 μm in inner diameter, and about 12 cm in length). Second, the spinning dopes went through the duct and flowed into the pure tap-water in a glass water tank, immediately solidifying and spontaneously rising to form the initial fibers. If the spinning dopes received a sudden rotating force in the tap-water, they would helically rise to form the initial helical fibers. Third, after the initial fibers freely rose from underwater to water surface and stayed for about 3 min in the tap-water, they were taken out of the water tank, and received

Table 1 Composition of the spinning dopes used for the biomimetic preparation of the elastomeric fibers.

Mass ratio (nanoparticle/TPU)	0/20	1/20	2/20	3/20	4/20	5/20
m_1 (g)	2	2	2	2	2	2
m_2 (g)	0	0.1	0.2	0.3	0.4	0.5
v_1 (mL)	15	15	15	15	15	15
v_2 (mL)	5	5	5	5	5	5
c (g/mL)	0.100	0.105	0.110	0.115	0.120	0.125

Notes: m_1 and m_2 denote the masses of TPU and nanoparticles, respectively; v_1 and v_2 denote the volumes of DMF and ethanol; c denotes the mass concentration of spinning dopes; $c = (m_1 + m_2) / (v_1 + v_2)$.

vertical stretching up to 2–5 times of the initial length in another water tank full of tap-water for about 40 min, and then the stretched fibers were achieved. Fourth, the stretched fibers were dried for about 12 h at 45 °C under vacuum for obtaining the final fibers. The initial helical fibers, without vertical stretching in the tap-water, were directly dried in the same conditions for getting the final helical fibers.

2.4. SEM observation on the fibers

SEM observation on the surfaces and cross-sections of the fibers was conducted with a field-emission scanning electron microscopy (HITACHI-S4800, Japan). The cross-sections of the fibers were achieved by slowly stretching the fibers to break. All the specimens were coated with gold before testing.

3. Results and discussion

3.1. Biomimetic preparation and formation mechanism of the fibers

The preparation of the native spider silks was divided into three steps [15,26,35]: first, highly concentrated protein solutions (spinning dopes with water as solvents, up to 0.50 g/mL in concentration) were produced and stored in the lumen of silk glands; second, the protein solutions flowed into a native tapering spinning duct, and simultaneously started self-assembling to form an initial silk in the duct, accompanied by the extraction of water solvents, ion exchange, shift of pH, and shear force; third, the initial silk was extruded out of the duct into the air, subsequently stretched and dried in the air to remove the residual water, and a protein nano-crystalline reinforced dragline silk or a periodically helical capture silk was finally made. The formation mechanism of the native spider silks was simply considered as a self-assembly mechanism, mainly originating from the process that the silk proteins, being driven by hydrogen bonding and hydrophobic action, self-assembled into β -sheets and further assembled into soft micelles (10–100 nm in diameter). Actually, the formed soft micelles were further transformed, which finally caused the emerging of the multi-scale microstructures on and in the native spider silks [26]. More accurately, the formation mechanism of the native spider silks was an integrated mechanism of diffusion, coagulation, self-assembly, and microphase separation [34].

In our biomimetic preparation, we hoped the added nanoparticles (nano-SiO₂ or UFPNBR), like the protein micelles (about 10–100 nm in diameter) formed in the production of the native spider silks [26], together with the TPU macromolecules to self-assemble into multi-scale microstructures on or in the nanoparticle/TPU

elastomeric fibers. It was noted that the self-assembly of the silk proteins and silk protein micelles mainly happened in the native tapering spinning duct of spiders, but in our artificial spinning duct, the self-assembly of the nanoparticles and TPU macromolecules was very hard to occur because of the lack of triggers such as the extraction of water solvents, ion exchange, shift of pH, and shear force [34]. Thus, in our biomimetic preparation of the nanoparticle/TPU fibers, the key problem was how to produce some triggers so as to activate the self-assembly of the nanoparticles and TPU macromolecules on and in the nanoparticle/TPU fibers.

In the previous study on the preparation of the UFPNBR/TPU fibers [34], some approaches had been adopted to activate the self-assembly of the UFPNBR nanoparticles and TPU macromolecules mainly on the UFPNBR/TPU fibers, such as the ethanol assistant processing [36], the fibers' formation in the pure tap-water, and the fibers' vertical stretching in the pure tap-water or in the air. As a result, the UFPNBR nanoparticles and TPU macromolecules self-assembled to form the multi-scale microstructures on the final UFPNBR/TPU fibers. The formation mechanism of the UFPNBR/TPU fibers was thought as an integrated mechanism of diffusion, coagulation, self-assembly, and microphase separation, same as the formation mechanism of the native spider silks.

In the present study, those approaches to activate the self-assembly of the UFPNBR nanoparticles and TPU macromolecules on the UFPNBR/TPU fibers were adopted again so as to successfully prepare the nano-SiO₂/TPU fibers with distinctive multi-scale microstructures on and in the fibers. The nano-SiO₂ spheres with diameter of about 10 nm were smaller than the UFPNBR nanoparticles (about 100 nm in diameter), and the nano-SiO₂ spheres with diameter of about 100 nm were more hydrophilic (easier to be dispersed and suspended in water) than the UFPNBR nanoparticles, all which hinted that the self-assembly of the nano-SiO₂ spheres would be a little different from that of the UFPNBR nanoparticles on and in the final fibers. That was to say, the final multi-scale microstructures on and in the nano-SiO₂/TPU fibers would be unique. Though the nano-SiO₂ spheres differed a bit from the UFPNBR nanoparticles in diameter and hydrophilicity, which necessarily caused some differences in the multi-scale microstructures of the fibers, the formation mechanism of the nano-SiO₂/TPU fibers was still inferred to be the integrated mechanism of diffusion, coagulation, self-assembly, and microphase separation because of the same preparation method and similar solution system.

3.2. External microstructures of the fibers

Fig. 1 is the SEM images of the nano-SiO₂/TPU elastomeric fibers with different microstructures on the surface. Image a, b, and c showed the first kind of the fibers with the nano-SiO₂ spheres with diameter of about 10 nm (scale bars: a—100 μ m, b—10 μ m,

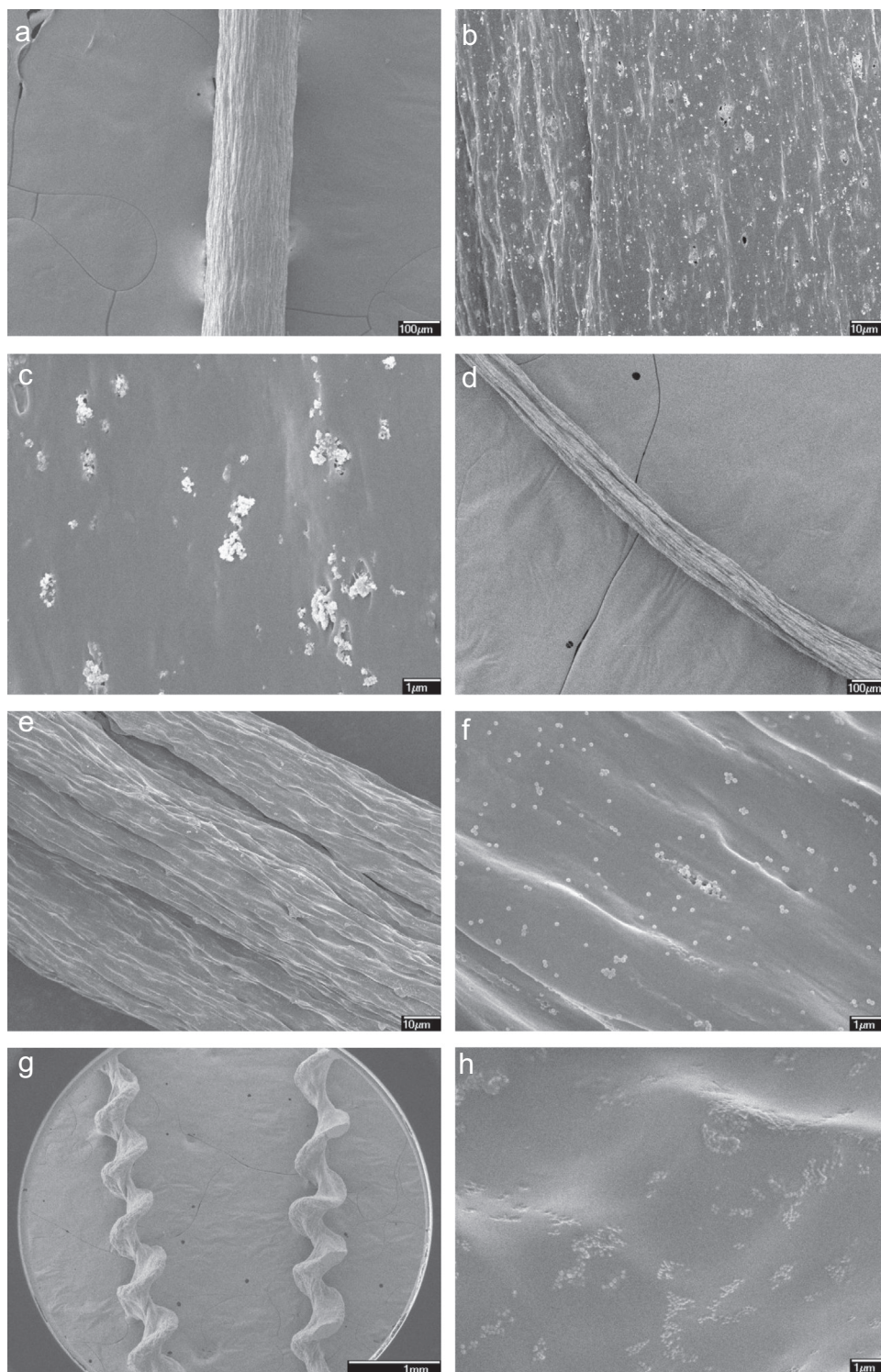


Fig. 1 SEM images of the nano-SiO₂/TPU elastomeric fibers with different microstructures on the surface.

c—1 μm). Image d, e, and f displayed the second kind of the fibers with the nano-SiO₂ spheres with diameter of about 100 nm (scale bars: d—100 μm , e—10 μm , f—1 μm). Image g and h illustrated the helical fibers with the nano-SiO₂ spheres with diameter of about 100 nm (scale bars: g—1 mm, h—1 μm). All the mass ratios of nano-SiO₂ to TPU were 3/20.

The first kind of nano-SiO₂/TPU fibers (Fig. 1a–c; about 200 μm in diameter) were decorated by both the micron-sized grooves

(below 10 μm in width) and nano-SiO₂ aggregates (about 10–1000 nm in size, composed of the nano-SiO₂ spheres with diameter of about 10 nm) on the surface, and the micron-sized grooves (Fig. 1a and b) extending along the axis of the fibers were narrow and dense, but the nano-SiO₂ aggregates (Fig. 1c) were randomly distributed on the fibers. The second kind of nano-SiO₂/TPU fibers (Fig. 1d–f; about 100 μm in diameter) were dotted by both the micron-sized grooves (below 15 μm in width) and nano-SiO₂

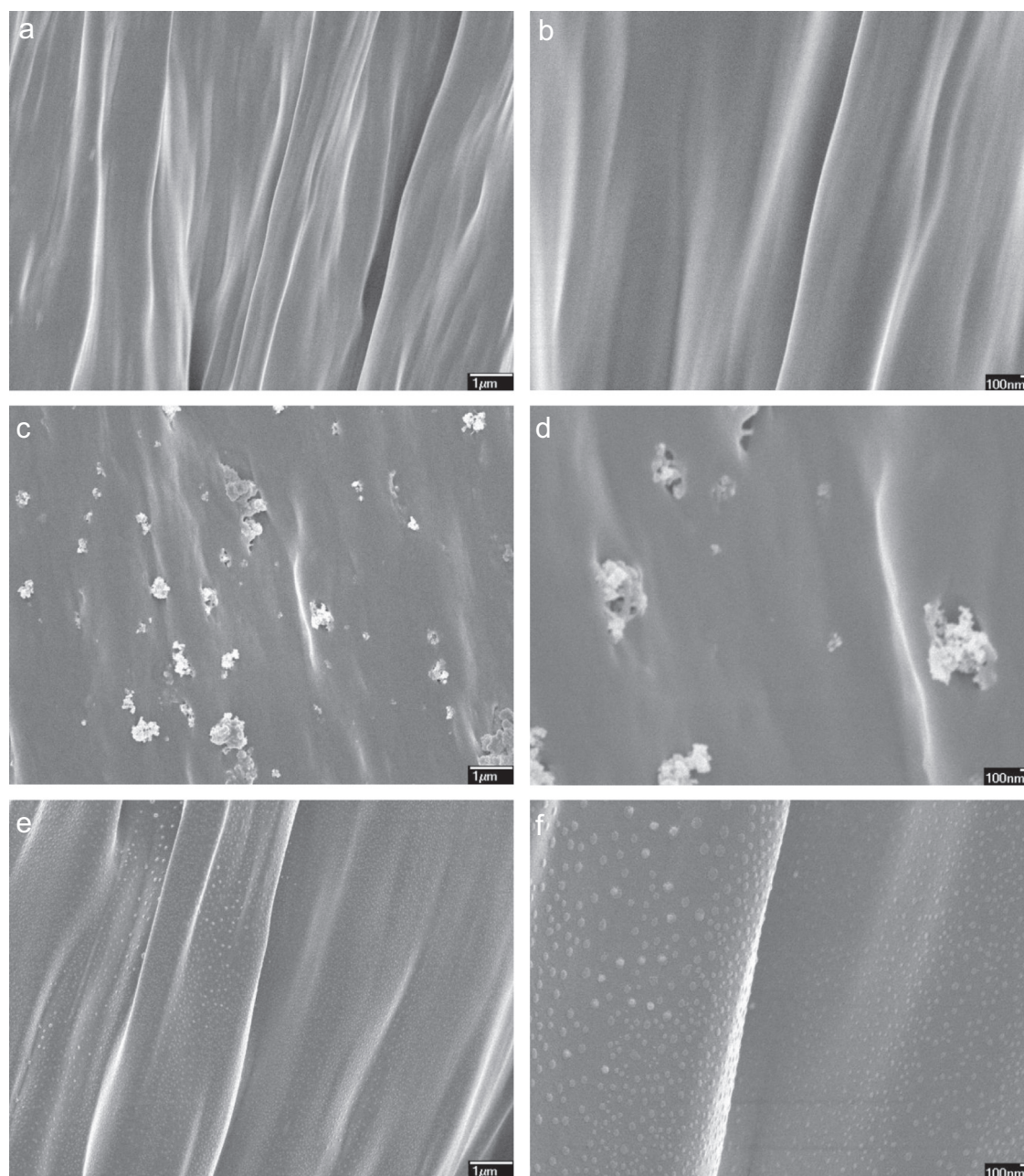


Fig. 2 SEM images of the surfaces of the pure TPU, nano-SiO₂/TPU, and UFPNBR/TPU elastomeric fibers.

spheres (about 100 nm in diameter) on the surface, and in comparison with the just mentioned micro-sized grooves (Fig. 1a and b), the present micro-sized grooves (Fig. 1d and e) seemed to be wider and sparser though they still extended along the axis of the fibers, but different from the nano-SiO₂ spheres with diameter of about 10 nm mostly aggregating on the fibers (Fig. 1c), most nano-SiO₂ spheres (Fig. 1f, about 100 nm in diameter) flatted and spread on the fibers. The third kind of nano-SiO₂/TPU fibers (Fig. 1g and h) were helical fibers (about 400 μm in screw diameter and pitch) presenting a concave-convex structure on the surface (Fig. 1h), and many nano-SiO₂ spheres (about 100 nm in diameter) were flatted and spread chunk by chunk on the fibers (Fig. 1h).

Here, the nano-SiO₂/TPU fibers (nano-SiO₂ spheres with diameter of about 10 nm, not discussing the helical fibers) were

specially compared with the pure TPU and UFPNBR/TPU elastomeric fibers in external microstructures, as shown in Fig. 2 which is the SEM images of the surfaces of the pure TPU, nano-SiO₂/TPU, and UFPNBR/TPU elastomeric fibers. Image a and b showed the surfaces of the pure TPU fibers without any nanoparticles added (scale bars: a—1 μm, b—100 nm). Image c and d displayed the surfaces of the nano-SiO₂/TPU fibers (nano-SiO₂ spheres with diameter of about 10 nm, mass ratio of nano-SiO₂ to TPU: 4/20, scale bars: c—1 μm, d—100 nm). Image e and f illustrated the surfaces of the UFPNBR/TPU fibers (UFPNBR nanoparticles with diameter of about 100 nm, mass ratio of UFPNBR to TPU: 4/20, scale bars: e—1 μm, f—100 nm).

Same as the pure TPU and UFPNBR/TPU fibers, the nano-SiO₂/TPU fibers were also dotted by the micron-sized grooves on

the surface. But different from the pure TPU fibers decorated only by the micron-sized grooves on the surface (Fig. 2a and b), the nano-SiO₂/TPU fibers were dotted by the nano-SiO₂ aggregates besides the micron-sized grooves on the surface (Fig. 2c and d), and also different from the UFPNBR/TPU fibers on which the UFPNBR nanoparticles (about 100 nm in diameter) could be very uniformly distributed (Fig. 2e and f), the nano-SiO₂/TPU fibers were dotted by the random nano-SiO₂ aggregates on the surface (Fig. 2c and d). Based on the previous study on the UFPNBR/TPU fibers [34], similarly, it was easily known that the TPU macromolecules self-assembled on the surface of the nano-SiO₂/TPU fibers so as to form the micro-sized grooves, and the microphase separation between the nano-SiO₂ and TPU macromolecules and the self-assembly of the nano-SiO₂ jointly resulted in the generation of the nano-SiO₂ aggregates on the nano-SiO₂/TPU fibers.

Why could the UFPNBR nanoparticles be very uniformly distributed on the UFPNBR/TPU fibers while the nano-SiO₂ aggregates or spheres were only randomly distributed on the nano-SiO₂/TPU fibers? The answer was hoped to be found in the nature of the used nanoparticles. On the one hand, the UFPNBR nanoparticles were relatively easy to be homogeneously dispersed in the TPU matrixes because they could be first swelled by the DMF in the TPU solutions and then presented a good compatibility with the TPU matrixes, though they were potentially easy to form the UFPNBR aggregates because of their high specific surface area and surface energy. Furthermore, the hydrophilicity of the UFPNBR nanoparticles was weaker so that the microphase separation between the UFPNBR and TPU macromolecules and the self-assembly of the UFPNBR on the UFPNBR/TPU fibers were partly restricted when the UFPNBR/TPU fibers were initially formed and subsequently stretched in the tap-water. That was to say, the UFPNBR nanoparticles tended to be partly separated from the TPU macromolecules on the interface of the water and fibers, and slowly self-assembled uniformly on the UFPNBR/TPU fibers. On the other hand, the nano-SiO₂ spheres were relatively easy to form the nano-SiO₂ aggregates because of their high specific surface area and surface energy, and were relatively difficult to be homogeneously dispersed in the TPU matrixes because they could not be swelled by the DMF in the TPU solutions and presented a bad compatibility with the TPU matrixes. Moreover, the hydrophilicity of the nano-SiO₂ spheres was stronger so that the microphase separation between the nano-SiO₂ and TPU macromolecules and the self-assembly of the nano-SiO₂ on the nano-SiO₂/TPU fibers were enhanced when the nano-SiO₂/TPU fibers were initially formed and subsequently stretched in the tap-water. That was to say, the nano-SiO₂ spheres tended to be completely separated from the TPU macromolecules on the interface of the water and fibers, and quickly self-assembled randomly on the nano-SiO₂/TPU fibers. Especially, in comparison with the nano-SiO₂ spheres with diameter of about 100 nm, the nano-SiO₂ spheres with diameter of about 10 nm had higher specific surface area and surface energy so that they were easier to form the nano-SiO₂ aggregates on the final fibers (Fig. 1c and f).

Furthermore, the influence of the mass ratios of nano-SiO₂ (about 10 nm in diameter) to TPU on the external microstructures of the nano-SiO₂/TPU fibers was particularly studied, as shown in Fig. 3 which is the SEM images of the nano-SiO₂/TPU elastomeric fibers at different mass ratios of nano-SiO₂ to TPU. Image a and b showed the surfaces of the nano-SiO₂/TPU fibers at the mass ratio of 1/20 (scale bars: a—100 μ m, b—1 μ m). Image c and d displayed the surfaces of the nano-SiO₂/TPU fibers at the mass ratio of 3/20 (scale bars: c—100 μ m, d—1 μ m). Image e and f

illustrated the surfaces of the nano-SiO₂/TPU fibers at the mass ratio of 5/20 (scale bars: e—100 μ m, f—1 μ m).

Overall, no matter whether the mass ratio of nano-SiO₂ to TPU was high or low, the surfaces of the nano-SiO₂/TPU fibers were always decorated by both the micron-sized grooves and nano-SiO₂ aggregates, which was different from the previous results that the surfaces of the UFPNBR/TPU fibers were only sometimes dotted by the UFPNBR nanoparticles besides the micron-sized grooves as the mass ratio of UFPNBR to TPU increased [34]. The nano-SiO₂ aggregates always existed on the nano-SiO₂/TPU fibers because of the strong hydrophilicity of the used nano-SiO₂ (Fig. 3b, d and f), and the number and size of the nano-SiO₂ aggregates on the fibers tended to become larger as the mass ratio of nano-SiO₂ to TPU increased. Additionally, it was noticed that, with the increase of the mass ratio of nano-SiO₂ to TPU, the nano-SiO₂/TPU fibers trended to present larger diameters (Fig. 3a and c) and smaller grooves (Fig. 3b and d) on the surface when the fibers were prepared in the same conditions, and the reason was thought as the stronger adsorption and filling ability of more nano-SiO₂ spheres to the TPU matrixes.

3.3. Inner microstructures of the fibers

Fig. 4 shows the SEM images of the cross-sections of the pure TPU and nano-SiO₂/TPU elastomeric fibers. Image a and b were corresponding to the pure TPU fibers without any nanoparticles added (scale bars: a—10 μ m, b—1 μ m). Image c and d were corresponding to the nano-SiO₂/TPU fibers (nano-SiO₂ with diameter of about 10 nm, mass ratio of nano-SiO₂ to TPU: 3/20, scale bars: c—1 μ m, d—100 nm). Image e and f were corresponding to the nano-SiO₂/TPU fibers (nano-SiO₂ with diameter of about 100 nm, mass ratio of nano-SiO₂ to TPU: 3/20, scale bars: e—1 μ m, f—100 nm).

The cross-sections of the pure TPU fibers were rough (Fig. 4a), which hinted that the tensile break of the fibers behaved as the mechanism of ductile fracture. Some microspheres (most about 1 μ m in diameter) were found to exist on the cross-sections of the pure TPU fibers, and these microspheres seemed to enjoy adhering together (Fig. 4b). But more microspheres (also most about 1 μ m in diameter) were found to exist on the cross-sections of the nano-SiO₂/TPU fibers (nano-SiO₂ with diameter of about 10 nm), and these microspheres seemed to be spaced apart by the nano-SiO₂ aggregates (Fig. 4c and d). However, no microspheres were found to exist on the cross-sections of the nano-SiO₂/TPU fibers (nano-SiO₂ with diameter of about 100 nm), while many nanospheres (actually being the nano-SiO₂ spheres) were found and seemed to be uniformly dispersed. How did the microspheres form in the TPU matrixes? Why did only some microspheres exist in the pure TPU fibers but more microspheres existed in the nano-SiO₂/TPU fibers (nano-SiO₂ with diameter of about 10 nm)? Why did the microspheres exist in the nano-SiO₂/TPU fibers (nano-SiO₂ with diameter of about 10 nm) while no microspheres existed in the nano-SiO₂/TPU fibers (nano-SiO₂ with diameter of about 100 nm)? In fact, here a serial of questions required to be explained.

First of all, it was easy to judge that the formed microspheres in the pure TPU and nano-SiO₂/TPU fibers were mainly composed of the TPU macromolecules, and the formation of these microspheres was due to the self-assembly of the TPU macromolecules. In the native spider dragline silks, the silk proteins could self-assemble into many nano-crystallines in the protein matrixes; similarly, in the present fibers, the TPU macromolecules self-assembled into

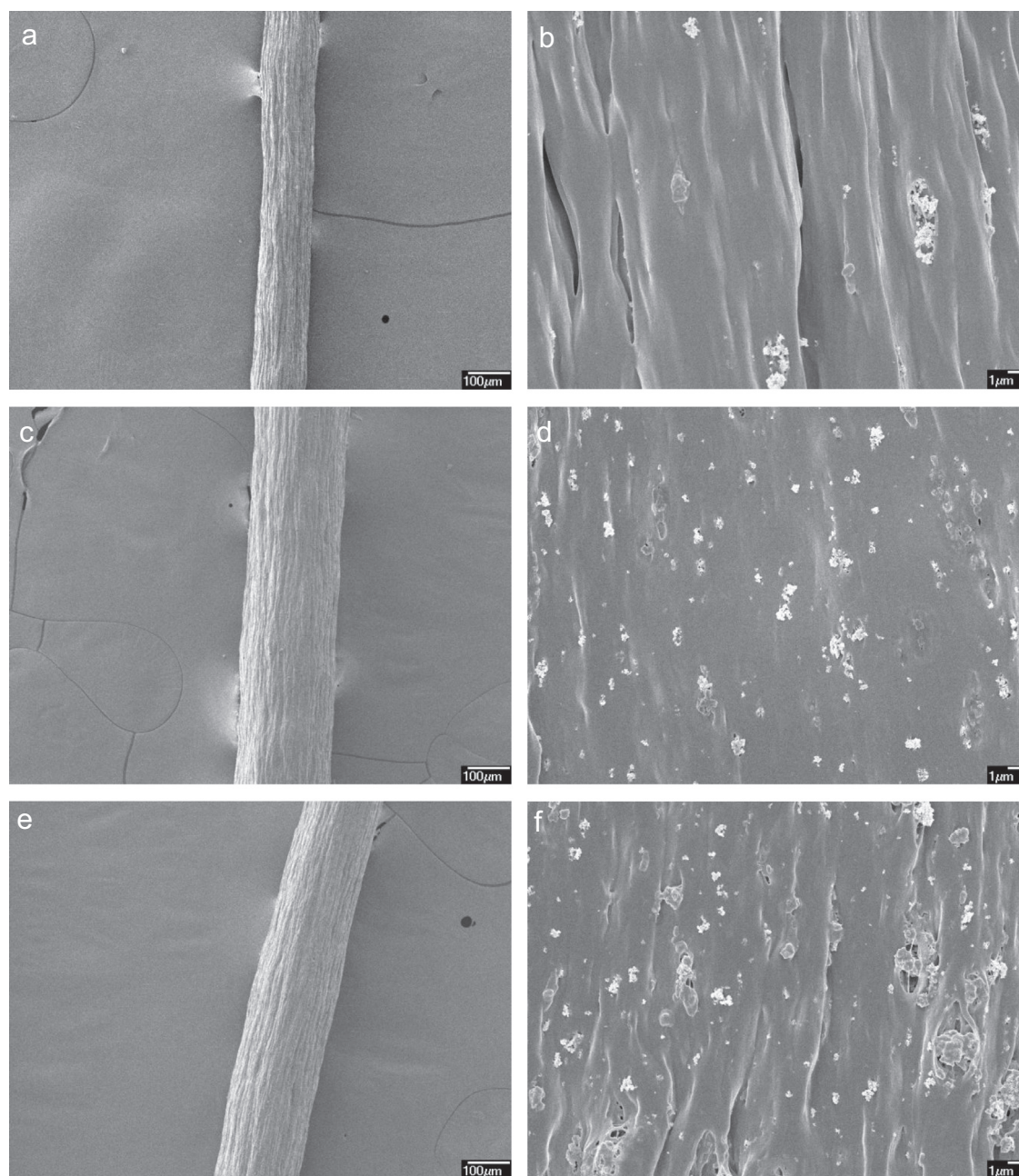


Fig. 3 SEM images of the nano-SiO₂/TPU elastomeric fibers at different mass ratios of nano-SiO₂ to TPU.

many microspheres in the TPU matrixes. How on earth did the TPU macromolecules self-assemble into the microspheres in the TPU matrixes? It was really a very interesting question. It was known that the DMF was a good solvent of TPU, so the adding of the DMF solvents destroyed the hydrogen bonding among the TPU macromolecules and further dissolved the TPU macromolecules; while the ethanol, same to the water, was a poor solvent of TPU, so the adding of the ethanol solvents made the TPU macromolecules tend to be precipitated from the DMF solvents. Thus, in the preparation of the spinning dopes, the adding of the ethanol solvents into the TPU solutions first resulted in the formation of a non-uniform two-phase (the DMF-dissolved TPU macromolecules and the ethanol-precipitated TPU macromolecules) structure, but after a stirring-mixing procedure the formed non-uniform two-phase structure finally became a new uniform

two-phase (the continuous phase of the DMF-dissolved TPU macromolecules and the dispersed phase of the ethanol-precipitated TPU macromolecules) structure. The TPU macromolecules, similar to the spider silk proteins, were segmented polymers, which hinted that the TPU macromolecules possibly self-assembled into varied shapes such as the microspheres; moreover, the ethanol solvents were sometimes used as a kind of simplest emulsifiers or co-emulsifiers in the preparation of latex particles. Thus, we thought the ethanol solvents acted as the emulsifiers in the TPU solutions to help the ethanol-precipitated TPU macromolecules self-assemble into the microspheres in the final TPU spinning dopes, and the ethanol solvents finally formed a layer of protective films on the microspheres. That was to say, the TPU-self-assembled microspheres had existed in the spinning dopes. The TPU-self-assembled microspheres in the spinning

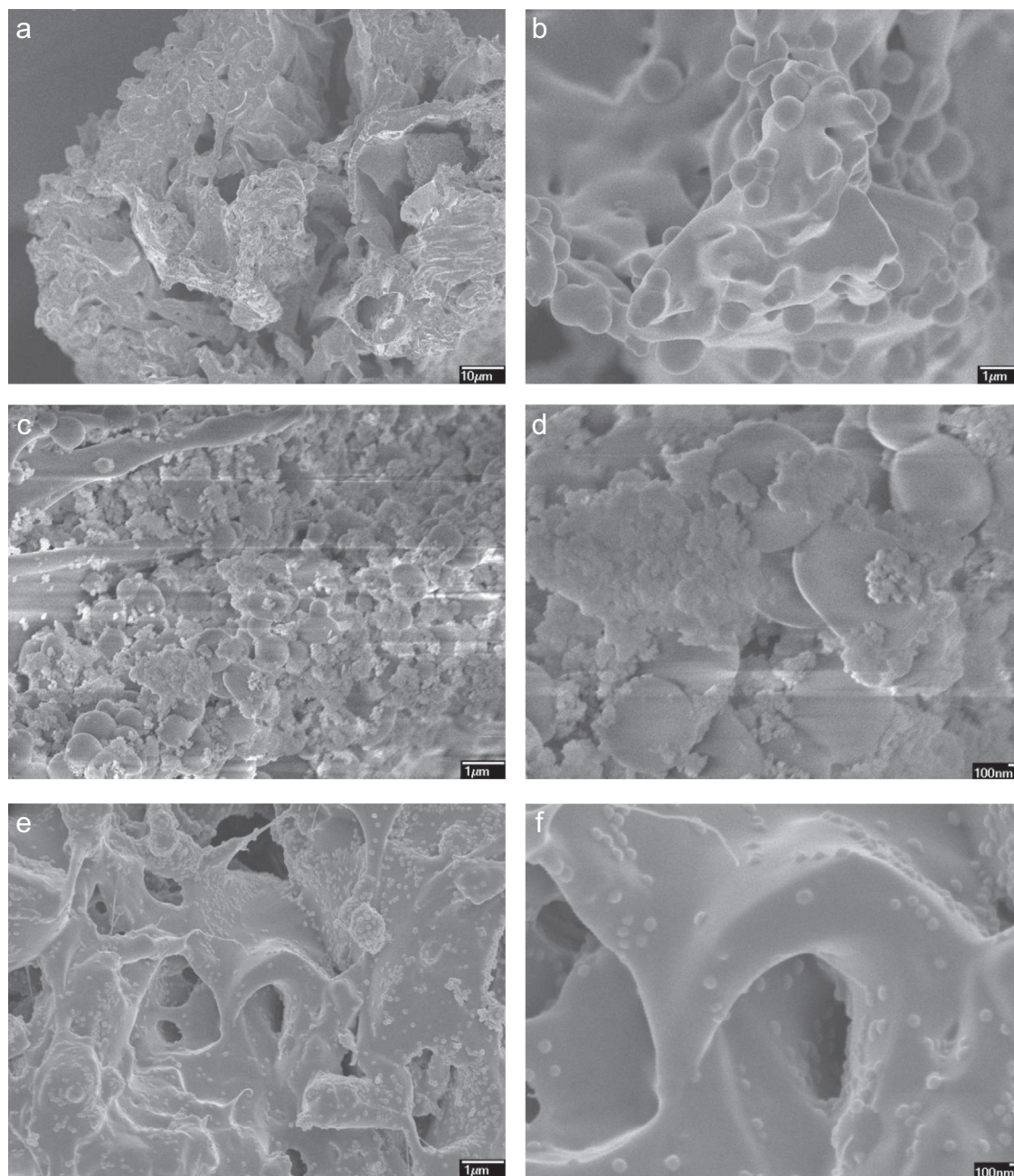


Fig. 4 SEM images of the cross-sections of the pure TPU and nano-SiO₂/TPU elastomeric fibers.

dopes could be further solidified and remained in the final pure TPU and nano-SiO₂/TPU fibers. But in the fibers' extrusion and vertical stretching procedure, some TPU-self-assembled microspheres were destroyed because of the external forces, and finally only part of the TPU-self-assembled microspheres were remained and some of them had adhered together, as shown in Fig. 4b. When the nano-SiO₂ spheres with diameter of about 10 nm, together with the ethanol solvents, were added into the TPU solutions, the nano-SiO₂ spheres, something like the ethanol emulsifiers, tended to promote the formation of the TPU-self-assembled microspheres in the spinning dopes and prevent the formed microspheres from being destroyed and adhering together under the extrusion and stretching forces; finally, many TPU-self-assembled microspheres were remained in the nano-SiO₂/TPU fibers and most of them had been spaced apart by the nano-SiO₂

aggregates, as displayed in Fig. 4d. However, when the nano-SiO₂ spheres with diameter of about 100 nm, together with the ethanol solvents, were added into the TPU solutions, the nano-SiO₂ spheres, something like the demulsifiers, tended to completely prevent the TPU-self-assembled microspheres from being formed in the spinning dopes, and finally only the nano-SiO₂ spheres were found in the nano-SiO₂/TPU fibers, as illustrated in Fig. 4f.

Moreover, the influence of the mass ratios of nano-SiO₂ (about 10 nm in diameter) to TPU on the inner microstructures of the nano-SiO₂/TPU fibers was particularly researched, as shown in Fig. 5 which is the SEM images of the cross-sections of the nano-SiO₂/TPU elastomeric fibers at different mass ratios of nano-SiO₂ to TPU. Image a showed the inner microstructures of the nano-SiO₂/TPU fibers at the mass ratio of 2/20 (scale bar: 10 μm). Images b, c, d, e, f respectively illustrated the inner microstructures

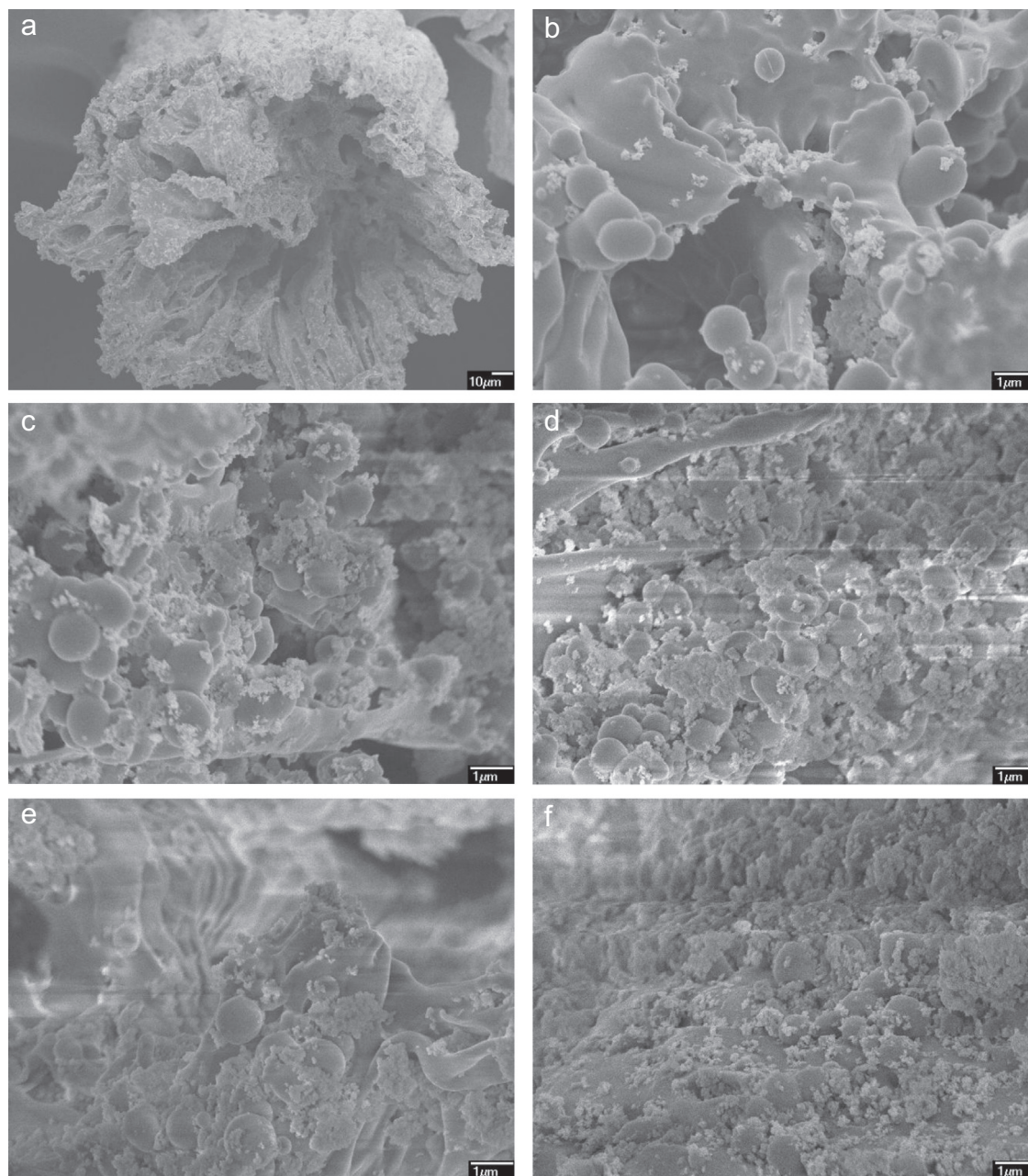


Fig. 5 SEM images of the cross-sections of the nano-SiO₂/TPU elastomeric fibers at different mass ratios of nano-SiO₂ to TPU.

of the nano-SiO₂/TPU fibers at the mass ratios of 1/20, 2/20, 3/20, 4/20, and 5/20 (scale bars: 1 μm).

Similar to the pure TPU fibers (Fig. 4a), all the nano-SiO₂/TPU fibers presented a rough cross-section structure (Fig. 5a), which indicated that the tensile break of the nano-SiO₂/TPU fibers also behaved as the mechanism of ductile fracture. On the cross-sections of all the nano-SiO₂/TPU fibers, the TPU-self-assembled microspheres spaced apart by the nano-SiO₂ aggregates were found, but the number of the microspheres tended to first rise and then decline as the mass ratio of nano-SiO₂ to TPU increased from 1/20 to 5/20 (Fig. 5b–f), and especially the number of the microspheres seemed to reach the maximum at the mass ratio of 3/20 (Fig. 5d). This hinted that only the certain number of the nano-SiO₂ added would guarantee lots of the TPU-self-assembled microspheres were remained in the final nano-SiO₂/TPU fibers,

while the smaller and larger number of the nano-SiO₂ added would result in less TPU-self-assembled microspheres remained in the final nano-SiO₂/TPU fibers. In other words, the relationship between the number of the remained TPU-self-assembled microspheres and the mass ratio of nano-SiO₂ to TPU seemed to agree with the Gaussian curve.

3.4. Formation process of the fibers with multi-scale microstructures

Based on the above observation and analysis about the external and inner microstructures of the pure TPU and nano-SiO₂/TPU elastomeric fibers, the formation process of the representative

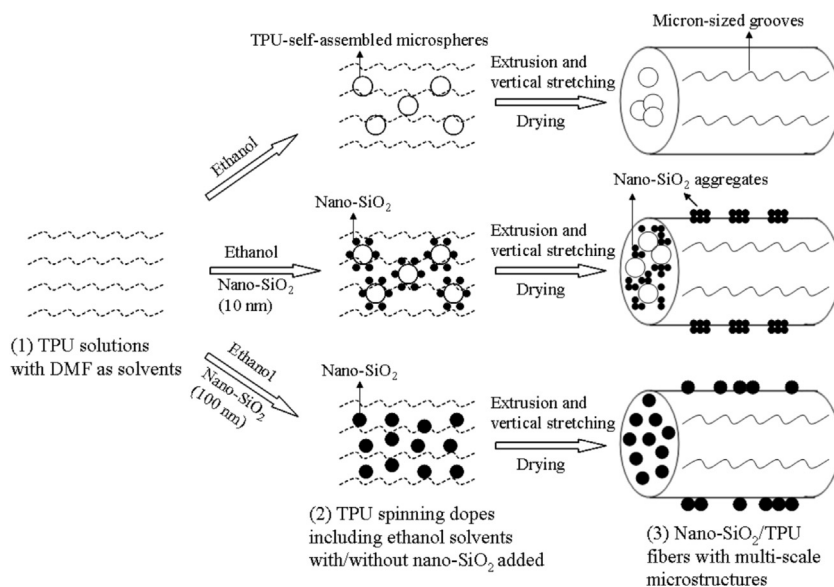


Fig. 6 Formation process of the pure TPU and representative nano-SiO₂/TPU elastomeric fibers with different multi-scale microstructures. (The mass ratios of nano-SiO₂ to TPU were 3/20, and most of the TPU-self-assembled microspheres were in diameter of about 1 μ m).

fibers with different multi-scale microstructures could be simply described as three main stages, as shown in Fig. 6. In the first stage, the TPU solutions with DMF as solvents were prepared, in which no other solvents and any nanoparticles were added. In the second stage, after some ethanol solvents with/without the nano-SiO₂ spheres were homogeneously blended into the prepared TPU solutions, the TPU-self-assembled microspheres were produced in both the pure TPU spinning dopes and the TPU spinning dopes including the nano-SiO₂ spheres with diameter of about 10 nm, while no TPU-self-assembled microspheres were produced in the TPU spinning dopes including the nano-SiO₂ spheres with diameter of about 100 nm. Moreover, in the TPU spinning dopes including the nano-SiO₂ spheres with diameter of about 10 nm, the nano-SiO₂ spheres were adsorbed around the surfaces of the TPU-self-assembled microspheres; but in the TPU spinning dopes including the nano-SiO₂ spheres with diameter of about 100 nm, only the nano-SiO₂ spheres were uniformly distributed. In the third stage, after the extrusion of the TPU spinning dopes into the tap-water to form the initial fibers, and then vertical stretching of the formed initial fibers in the tap-water, and finally drying of the stretched fibers in the vacuum oven, the pure TPU and nano-SiO₂/TPU fibers with different external and inner microstructures were achieved. On the pure TPU fibers, only the micron-sized grooves were produced, and in the pure TPU fibers, only some TPU-self-assembled microspheres were remained and part of them adhered together. However, on the nano-SiO₂/TPU fibers (nano-SiO₂ with diameter of about 10 nm), besides the micron-sized grooves, many nano-SiO₂ aggregates were adsorbed, and in the nano-SiO₂/TPU fibers, many TPU-self-assembled microspheres were remained and most of them were spaced apart by the nano-SiO₂ aggregates; furthermore, on the nano-SiO₂/TPU fibers (nano-SiO₂ with diameter of about 100 nm), besides the micron-sized grooves, many nano-SiO₂ spheres flatted and spread, and in the nano-SiO₂/TPU fibers, no TPU-self-assembled microspheres existed and only the nano-SiO₂ spheres seemed to be uniform distributed. As a result, the second stage, such as the adding of the ethanol solvents and nano-SiO₂ spheres in different diameters, seemed to be very crucial for the final external and inner microstructures of the prepared elastomeric fibers.

4. Conclusions

In this work, the biomimetic preparation of the nano-SiO₂/TPU elastomeric fibers (including the helical nano-SiO₂/TPU fibers) with different multi-scale microstructures was successfully implemented, and the formation mechanism of the fibers was considered as the integrated mechanism of diffusion, coagulation, self-assembly, and microphase separation. The nano-SiO₂/TPU fibers were dotted by the nano-SiO₂ aggregates or spheres randomly distributed on the surface. In the pure TPU fibers, some TPU-self-assembled microspheres were produced and part of them adhered together; but in the nano-SiO₂/TPU fibers (nano-SiO₂ spheres with diameter of about 10 nm), many TPU-self-assembled microspheres were produced and most of them were spaced apart by the nano-SiO₂ aggregates, and in the nano-SiO₂/TPU fibers (nano-SiO₂ spheres with diameter of about 100 nm), only the nano-SiO₂ spheres were found to be uniformly distributed. As the mass ratio of nano-SiO₂ (about 10 nm in diameter) to TPU increased, the number and size of the nano-SiO₂ aggregates on the nano-SiO₂/TPU fibers tended to rise, but the number of the TPU-self-assembled microspheres in the nano-SiO₂/TPU fibers tended to first rise and then decline, and the number of the TPU-self-assembled microspheres reached the maximum at the mass ratio of 3/20. The formation process of the nano-SiO₂/TPU fibers with different multi-scale microstructures was simply described as three main stages, and the second stage, such as the adding of the ethanol solvents and nano-SiO₂ spheres with different diameters, was very crucial for the formation of the external and inner microstructures of the final fibers.

Acknowledgments

This work was supported by National Science Foundation for Young Scientists of China (51003003), National Natural Science Foundation of China (21234001), National Research Fund for Fundamental Key Project (2013CB933000 and 2010CB934700), and Doctoral Fund of Ministry of Education of China (20121102110035). Authors thank Prof. Jinliang Qiao and Prof.

Xiaohong Zhang for supplying the nanoparticles of ultrafine full-vulcanized powdered nitrile-butadiene rubbers.

References

- [1] A.M. Kushner, Z.B. Guan, *Angew. Chem.-Int. Ed.* 50 (39) (2011) 9026–9057.
- [2] L. Eadie, T.K. Ghosh, J. R. Soc. Interface 8 (59) (2011) 761–775.
- [3] X.J. Liu, Y.M. Liang, F. Zhou, W.M. Liu, *Soft Matter* 8 (7) (2012) 2070–2086.
- [4] H.B. Yao, H.Y. Fang, X.H. Wang, S.H. Yu, *Chem. Soc. Rev.* 40 (7) (2011) 3764–3785.
- [5] K.S. Liu, L. Jiang, *Nano Today* 6 (2) (2011) 155–175.
- [6] H.Y. Erbil, A.L. Demirel, Y. Avci, O. Mert, *Science* 299 (5611) (2003) 1377–1380.
- [7] E. Munch, M.E. Launey, D.H. Alsem, E. Saiz, A.P. Tomsia, R.O. Ritchie, *Science* 322 (5907) (2008) 1516–1520.
- [8] Q.Y. Liu, L. Jiang, *Chem. J. Chinese U.* 31 (6) (2010) 1065–1071.
- [9] F.G. Omenetto, D.L. Kaplan, *Science* 329 (5991) (2010) 528–531.
- [10] Q.Y. Liu, L. Jiang, R. Shi, L.Q. Zhang, *Prog. Polym. Sci.* 37 (5) (2012) 715–765.
- [11] A. Miserez, S. ScottWasko, C.F. Carpenter, J.H. Waite, *Nat. Mater.* 8 (11) (2009) 910–916.
- [12] F. Vollrath, D. Porter, *Soft Matter* 2 (5) (2006) 377–385.
- [13] M. Heim, L. Romer, T. Scheibel, *Chem. Soc. Rev.* 39 (1) (2010) 156–164.
- [14] L. Eisoltd, A. Smith, T. Scheibel, *Mater. Today* 14 (3) (2011) 80–86.
- [15] J.G. Hardy, L.M. Romer, T.R. Scheibel, *Polymer* 49 (20) (2008) 4309–4327.
- [16] S. Kubik, *Angew. Chem.-Int. Ed.* 41 (15) (2002) 2721–2723.
- [17] Y.M. Zheng, H. Bai, Z.B. Huang, X.L. Tian, F.Q. Nie, Y. Zhao, J. Zhai, L. Jiang, *Nature* 463 (7281) (2010) 640–643.
- [18] Y. Liu, Z.Z. Shao, F. Vollrath, *Nat. Mater.* 4 (12) (2005) 901–905.
- [19] M. Heim, D. Keerl, T. Scheibel, *Angew. Chem.-Int. Ed.* 48 (20) (2009) 3584–3596.
- [20] J. Perez-Rigueiro, M. Elices, G.V. Guinea, *Polymer* 44 (13) (2003) 3733–3736.
- [21] S.P. Kelly, A. Sensenig, K.A. Lorentz, T.A. Blackledge, *Zoology* 114 (4) (2011) 233–238.
- [22] O. Emile, A. Le Floch, F. Vollrath, *Nature* 440 (7084) (2006) 621.
- [23] L. Pelit, F.N. Ertas, A.E. Eroglu, T. Shahwan, H. Tural, *Bioresour. Technol.* 102 (19) (2011) 8807–8813.
- [24] R.V. Lewis, *Chem. Rev.* 106 (9) (2006) 3762–3774.
- [25] X.P. Huang, G.Q. Liu, X.W. Wang, *Adv. Mater.* 24 (11) (2012) 1482–1486.
- [26] J.A. Kluge, O. Rabotyagova, G.G. Leisk, D.L. Kaplan, *Trends Biotechnol.* 26 (5) (2008) 244–251.
- [27] A.B. Dalton, S. Collins, E. Munoz, J.M. Razal, V.H. Ebron, J.P. Ferraris, J.N. Coleman, B.G. Kim, R.H. Baughman, *Nature* 423 (6941) (2003) 703.
- [28] S.M. Liff, N. Kumar, G.H. McKinley, *Nat. Mater.* 6 (1) (2007) 76–83.
- [29] Q.J. Wu, M. Henriksson, X. Liu, L.A. Berglund, *Biomacromolecules* 8 (12) (2007) 3687–3692.
- [30] P. Podsiadlo, E.M. Arruda, E. Kheng, A.M. Waas, J. Lee, K. Critchley, M. Qin, E. Chuang, A.K. Kaushik, H.S. Kim, Y. Qi, S.T. Noh, N.A. Kotov, *ACS Nano* 3 (6) (2009) 1564–1572.
- [31] S.M. Lee, E. Pippel, U. Gosele, C. Dresbach, Y. Qin, C.V. Chandran, T. Brauniger, G. Hause, M. Knez, *Science* 324 (5926) (2009) 488–492.
- [32] H. Bai, X.L. Tian, Y.M. Zheng, J. Ju, Y. Zhao, L. Jiang, *Adv. Mater.* 22 (48) (2010) 5521–5525.
- [33] X.L. Tian, H. Bai, Y.M. Zheng, L. Jiang, *Adv. Funct. Mater.* 21 (8) (2011) 1398–1402.
- [34] Q.Y. Liu, L.Q. Zhang, L. Jiang, *Prog. Nat. Sci.: Mater. Int.* 22 (5) (2012) 493–501.
- [35] F. Vollrath, D.P. Knight, *Nature* 410 (6828) (2001) 541–548.
- [36] Q.Y. Liu, J.Y. Wu, T.W. Tan, L.Q. Zhang, D.F. Chen, W. Tian, *Polym. Degrad. Stabil.* 94 (9) (2009) 1427–1435.